Treatment with spermidine alleviates the effects of concomitantly applied cold stress by modulating Ca2+, pH and ROS homeostasis, actin filament organization and cell wall deposition in pollen tubes of Camellia sinensis

Treatment with spermidine alleviates the effects of concomitantly applied cold stress by modulating Ca^{2+}, pH and ROS homeostasis, actin filament organization and cell wall deposition in pollen tubes of *Camellia sinensis*

Aslıhan Çetinbaş-Genç*[a], Giampiero Cai[b], Stefano Del Duca[c]

[a]Department of Biology, Marmara University, Göztepe Campus, Kadıköy, 34722, Istanbul, Turkey

[b]Department of Life Sciences, University of Siena, via Mattioli 4, 53100, Siena, Italy

[c]Department of Biological, Geological and Environmental Sciences, University of Bologna, via Irnerio 42, 40126 Bologna, Italy

E-mails of the authors: giampiero.cai@unisi.it

stefano.delduca@unibo.it

*Corresponding author:

ORCID ID: 0000-0001-5125-9395

E-mail: aslihan.cetinbas@marmara.edu.tr

Mail: Department of Biology, Marmara University, Göztepe Campus, 34722 Istanbul, Turkey

Mobile phone: + 90 530 230 42 87

Fax: + 90 216 347 87 83

Highlights

- Spermidine (Spd) alleviates cold-induced changes in pollen tubes under cold stress
- Spd promotes pollen germination and tube growth under cold stress
- Spd ameliorates the cold-induced changes in actin organization under cold stress
- Spd ameliorates the cold-induced changes in callose distribution under cold stress
- Spd alleviates the cold-induced changes in Ca2+, pH, ROS under cold stress

Abstract

The aim of the current study was to examine the effect of spermidine treatment concomitant with cold stress on the elongation of *Camellia sinensis* pollen tube. When exogenous spermidine (0.05 mM) was applied concomitantly with cold stress, pollen germination rate and pollen tube length were significantly increased in comparison with cold stressed pollen tubes. In addition, spermidine treatment concomitantly with cold stress reduced pollen tube abnormalities induced by cold stress. Besides, cold-induced disorganizations of actin filaments were ameliorated after spermidine treatment along with cold stress because anisotropy levels of actin filaments in shank and apex of pollen tubes decreased. Changes in cold-induced callose distribution in the pollen tube cell wall were partially recovered after spermidine/cold stress treatment. Other cold-induced effects (decrease in Ca^{2+} content, reduction of pH gradient, accumulation of ROS) were reverted to adequate levels after spermidine treatment in conjunction with cold stress, indicating that pollen tubes are able to cope with stress. Thus, spermidine treatment reorganized the growth pattern of pollen tubes by modulating Ca^{2+} and ROS homeostasis, actin cytoskeleton organization, and cell wall deposition in *Camellia sinensis* pollen tubes under cold stress.

Key words: Actin cytoskeleton; Cell wall; Cold stress; Pollen tube; Polyamines; Spermidine

1. Introduction

Camellia sinensis (L.) O. Kuntze. (tea) is an evergreen, perennial plant belonging to the Theaceae family, which also contains about 600 species (Pascoa et al., 2019; Bora et al., 2019). No doubt it is an important plant due to its huge industrial, cultural, and medicinal applications (Zhan et al., 2019), and alsoit has high economic value because leaves are used in the tea beverage production and the oil obtained from seeds is used in food and cosmetics industry (Yu and Yang, 2019). Because of its high cultural and economic value, it is cultivated in many countries, especially in China, India, Srilanka, Kenya and Turkey (Haq and Boz, 2018, Yu and Yang, 2019). Tea is grown worldwide in various agro-climatic regions, including cold ones (Pan et al., 2016; Li et al., 2018). However, cold stress is one of the major abiotic stresses that limits the development, productivity, and seed formation of tea plants (Pan et al., 2016; Wang et al., 2016). Reproductive processes, especially pollen germination and pollen tube elongation, are highly vulnerable to cold stress (Wang et al., 2016; Parrotta et al., 2019).

Angiosperm pollen tubes elongate by rapid tip growth. Vesicles containing newly synthesized cell wall materials are transported to the tube tip by actin filaments thereby allowing pollen tubes to elongate and to maintain their cylindrical shape (Cai et al., 2015). According to actin filament organization, pollen tubes can be divided into 3 different zones: apex, sub-apex, and shank (Cai et al., 2010). In the shank, actin filaments are organized as long parallel bundles, allowing organelles and vesicles to be transported over long distances while they often form a

fringe-like structure in the sub-apex in which existing actin filaments are elongated or new ones are formed (Cai et al., 2015). Short and highly dynamic actin filaments characterize the tube apex. Since the apical region of pollen tubes include numerous regulatory factors (such as Ca^{+2}, reactive oxygen species [ROS], and actin-binding proteins) necessary for tube elongation, this region is considered a control center for making decisions about the direction and speed of pollen tube growth (Zonia, 2010). Therefore, actin filaments in the apex are very dynamic to quickly fit the new growth conditions and their dynamics is crucial to the proper tube elongation (Cai et al., 2015). This differential organization is controlled by actin-binding proteins (ABP) (Re and Xiang, 2007; Chen et al., 2018). Actin filaments also control the deposition of the cell wall in multiple ways; for example, actin filaments help to regulate the positioning and perhaps also the activity of sucrose synthase, the enzyme that breaks down sucrose to produce UDP-glucose for the synthesis of cellulose and callose (Persia et al., 2008). Callose is the most abundant polysaccharide of the pollen tube cell wall while cellulose is less abundant than callose in the pollen tube cell wall. Callose and cellulose are synthesized by, respectively, callose synthase and cellulose synthase in the plasma membrane. (Li et al., 1997; Doblin et al., 2001; Goubet et al., 2003).Even the localization of these two enzymes in the plasma membrane is likely controlled by actin filaments and partially by microtubules (Cai et al., 2011). These few examples already suggest that actin filaments are crucial in some processes essential for the pollen tube growth, such as the transport of vesicles and organelles and the correct synthesis of the cell wall.

Actin filament organization is also controlled by other direct or indirect factors. Actin filaments have a cross-talk with myosins used for the rapid and long-distance transport of membrane-bounded structures (such as vesicles and endoplasmic reticulum). (McCurdy, 1999; Cai et al., 2011). Myosin activity is dependent on the Ca^{2+}-gradient at the tube apex (Cai et al., 2011). In addition, proper accumulation of ROS at the tube apex contributes to regulate the free cytosolic Ca^{2+}-gradient by modulating Ca^{2+} channels (Lassig et al., 2014). Both under normal growing conditions and under stressful situations, the content of ROS at the apex changes and accordingly the relative concentration of Ca^{2+} in the apex also changes; this cross-talk between Ca^{2+} and ROS can help to counteract the effects of stressful conditions (Potocky et al., 2012; Kaya et al., 2014). Moreover, proper pH gradient within the tube is also related to the proper polymerization and orientation of actin filaments (Holdaway-Clarke and Hepler, 2003). Generally, the tube apex has slightly acidic pH values while the sub-apex and shank have an alkaline pH (Wilkins et al., 2015; Winship et al., 2017). The different distribution of pH within the tube is likely necessary for proper tube growth because it can help regulate the activity of some ABPs. Thus, each of the features given above is interrelated, and alteration to one of those features interferes with pollen tube elongation.

The effect of cold stress on pollen germination and tube elongation has been investigated in many species, including tea. Cold stress negatively affects pollen germination, tube elongation and tube shaping in *Cicer arietinum* (Srinivasan et al., 1999), *Pyrus persica* (Hedhly et al., 2005), *Pyrus bretschneideri* (Gao et al., 2014), *Dimocarpus longan* (Pham et al., 2015), *Prunus dulcis* (Sorkheh et al., 2018), *Cocos nucifera* (Hebbar et al., 2018) and *Corylus avellana* (Çetinbaş-Genç et al., 2019a). Wu et al. (2012) reported the cold-induced depolymerization of the actin cytoskeleton in pollen tubes of *Pyrus pyrifolia*. Wang et al. (2016) stated that cold stress disrupts the cytoplasmic Ca^{2+}-gradient, increases the ROS content and acidity of pollen tubes in *Camellia sinensis*. Cold stress negatively affects actin organization and cell wall distribution in pollen tubes of *Corylus avellana* cultivars

(Çetinbaş-Genç et al., 2019a). In addition, Parrotta et al. (2019) reported that cold stress interferes with cell wall deposition and Ca^{2+}-gradients, thereby changing the growth pattern of *Nicotiana tabacum* pollen tubes.

Plant growth regulators (PGR), such as flavanol, boron, gibberellic acid, and polyamines, are known to sustain the growth of pollen tubes when exposed to various stresses (Voyiatzsis et al., 2005). Among the most effective PGR molecules are polyamines (PA) whose omeostasisis critical at distinct stages of the pollen life span (Aloisi et al., 2016a). PA are small aliphatic polycations with low molecular weight and are present within the cell in free or bound form and their effects are multifactorial (Zhan et al., 2019). PA achieve their biological activity through their polycationic backbones that can establish electrostatic interactions with different anion groups of various biological molecules such as proteins, nucleic acids, and membrane phospholipids. In addition to their electrostatic interactions, they may also affect protein functionality because they covalently bind to glutamyl residues of specific proteins by transglutaminase-catalyzed reactions (Aloisi et al., 2016b). PA, when connected to actin and tubulin in pollen tubes, could affect the activity of the pollen tube cytoskeleton, and also they can be effective in pollen tube elongation because they bind to and affect the activity of motor proteins (Aloisi et al., 2016a). Besides, given that the most of cellular spermidine (Spd) is localized in the cell wall compartment (Bokern et al., 1995), PA could change the cell wall properties by interacting with different molecules (Charnay et al., 1992; Del Duca et al., 2009). The linkage of PA to phenylpropanoids gives rise to phenolamides, specialized metabolites present in reproductive organs and involved in pollen cell wall organization and therefore in fertilization (Grienenberger et al., 2009; Elejalde-Palmett et al., 2015). Among them, the trihydroxycinnamoyl Spd is a component of the tryphine, a constituent of the pollen coat involved in pollination and in pollen-stigma interaction (Grienenberger et al., 2009).

The effects of exogenous PA on cells can vary depending on the type and dose of PA (Aloisi et al., 2016a). In plants, the most common PA are putrescine (Put), spermine (Spm), and Spd (Del Duca et al., 2009). Although there are various studies on the effect of Put and Spm on pollen tube growth, little is known about the effects and mechanisms of action of Spd, the latter probably playing a key role in the protection of cell walls and nucleic acids under various stresses (Alvarez et al., 2003; Erland et al., 2014).

Effects of exogenous PA supplementation have been studied in *Solanum lycopersicum* (Song et al., 1999), *Helianthus annuus* (Çetin et al., 2000), *Pyrus serotine* (Dixin and Shaoling, 2002), *Prunus mume* (Wolukau et al., 2004), *Arabidopsis thaliana* (Wu et al., 2010) , *Prunus dulcis* (Sorkheh et al., 2011), *Pyrus communis* (Aloisi et al., 2015), *Camellia sinensis* (Çetinbaş-Genç et al. 2019), *Corylus avellana* (Çetinbaş-Genç et al., 2019b). Exogenous PA improved pollen tube elongation in a dose-dependent manner. In *Arabidopsis thaliana*, addition of exogenous Spd changed cytosolic free Ca^{2+} concentration, as well as H_2O_2 and ROS accumulation (Wu et al., 2010). Following the observation that PA has a protective effect in pollen tubes, exogenous PA treatments are reported to reduce damages caused by different temperature stresses in pollen tubes (Wolukau et al., 2004; Sorkheh et al., 2011). For example, damage caused by temperature stress can be ameliorated by PA supply in *Prunus dulcis* pollen tube (Sorkheh et al., 2011). Spm application can also protect plants against heat stress by increasing the expression of heat shock-related genes in *Arabidopsis thaliana* (Sagor et al., 2013). However, there is no detailed study explaining how PA application can compensate for the damage caused by cold stress in pollen tubes.

In the current study, we have examined the mitigating effect of Spd when added to *Camellia sinensis* growing pollen tubes simultaneously exposed to cold stress. Specifically, we focused on the actin cytoskeleton dynamics, the deposition of cell wall components, the Ca^{2+}-gradient distribution, the accumulation of ROS and on the acidity level. Our results can help understanding the complex cytological and biochemical process of pollen tube elongation under cold stress and the alleviating effects of Spd on cold-induced changes. Managing to reduce the negative effects of cold stress by the application of PA can be important to increase the pollination process and therefore reproduction in plants subjected to cold stress conditions or grown in colder areas of our planet.

2. Material and Methods

2.1. Plant material and in-vitro pollen culture

Pollen materials were collected from *Camellia sinensis* (L.) O. Kuntze. growing in the East Black Sea Region, Çayeli/Rize (Turkey) (41° 06′ 57.0″ N, 40° 45′ 27.0″ E). BK pollen culture medium containing 5% sucrose was used for germination assays (Brewbaker et al., 1963; Wang et al., 2016). Spd was used at concentrations determined according to previous studies (Song et al., 1999; Wolukau et al., 2004; Sorkheh et al., 2011; Aloisi et al., 2015). Pollen grains in the culture medium supplemented with 0.025, 0.05 or 0.1 mM Spd was incubated at 25 °C and Spd-free culture medium was used as control. For cold treatments, pollen grains were incubated at 4° C in Spd-free culture medium and in culture medium supplemented with 0.025, 0.05 or 0.1 mM Spd. All the germination processes were protracted for 3 hours in dark condition. Pollen grains were marked as germinated when tube lengths were higher than the diameter of pollen grains. All experiments were performed in triplicate and for each group; germination rates, lengths and tube abnormalities were measured by counting at least 150 pollen grains using an Olympus BX-51 light microscope equipped with KAMERAM software.

2.2. Labelling of actin filaments

Actin labelling was performed according to the Lovy-Wheeler method (Lovy-Wheeler et al., 2005). After 30 minutes of fixation with buffer (pH 6.9) containing 100 mM PIPES, 5 mM $MgSO_4$, 0.5 mM $CaCl_2$, 0.05% (v/v) Triton X-100, 1.5% (m/v) formaldehyde, and 0.05% (m/v) glutaraldehyde, pollen tubes were rinsed with the same buffer containing 10 mM EGTA, and 6.6 µM Alexa 488-phalloidin. Pollen tubes were visualized using an Olympus BX-51 fluorescence microscope with excitation at 488-nm and emission at 515-nm and equipped with KAMERAM software. For each treatment, images of different pollen samples were captured using same acquisition parameters and with one focal plane and 20 tubes with equal length were selected for all groups to analyze the anisotropy of actin filaments. Due to the sub-apex region represents a very small region of the pollen tube and it is very difficult to observe the actin fringe structure in the sub-apex region, actin filament anisotropy was measured at apex and shank regions. Actin filament anisotropy at the apex (arbitrarily measured for 10 µm segments from the apex) and shank zones were computed using the “Fibril Tool” plugin of ImageJ. Apex and shank zones are shown on figures as 'a' for apex and 's' for the shank. Anisotropy measurements were performed according to the method of Boudaoud et al. (2014). According to this method, the signal corresponding to fibrils was binarized (i.e., a pixel is given the value 1 if the signal is present and 0 if it is absent), and it provided an actin cytoskeleton of lines inside the cell that is amenable to analysis. With regard to the anisotropy score, the following convention was used: 0 for no order (purely isotropic arrays) and 1 for perfectly ordered, i.e., parallel fibrils (purely anisotropic arrays).

2.3. Labelling of cellulose and callose

To stain cellulose and callose, pollen tubes were incubated with calcofluor white and aniline blue, respectively (Lazzaro et al., 2003; Chen et al., 2007). Pollen tubes were visualized at 365-nm excitation and at 432-nm emission for calcofluor white (cellulose) and at 455-nm excitation and 495-nm emission for aniline blue (callose). For each treatment, images of different pollen samples were captured using same acquisition parameters and with one focal plane. To analyze the quantitative distribution of cellulose and callose in the pollen tube cell wall, normalized fluorescence intensity analysis was performed on 20 pollen tubes with equivalent length for each group. To estimate the accumulation of polysaccharide at the pollen tube apex, the normalized fluorescence intensity was measured in the area of the tube covering the first 10 µm from the apex using the "Rectangle Selection" tool of ImageJ and by subtracting the outer fluorescence background. The regions of interest (ROI) are shown on the figures. To assess the distribution of polysaccharides along the edge of pollen tubes, the fluorescence intensity measurement was conducted throughout the pollen tube cell wall, starting from the outermost tip of pollen tubes for 50 µm backwards using the "Segmented Line" tool of ImageJ with a selection width of about 4 µm. The segments are shown on the figures. Based on the average of 20 measurement results, representative graphics were created by ImageJ.

2.4. Imaging of Ca^{+2}, ROS and pH

For imaging of Ca^{2+}, ROS and pH, pollen tubes were incubated with Chlortetracycline hydrochloride (CTC), 5-(and 6-)chloromethyl-2′,7′-dichlorodihydrofluorescein diacetate (H_2DCFDA) and 2',7'-bis-(2-Carboxyethyl)-5-(and-6)-carboxyfluorescein acetoxymethyl ester (BCECF, AM), respectively (Fricker et al., 1997; Malho et al., 2000; Serrazina et al., 2014). Pollen tubes were visualized at 515-nm excitation and at 536-nm emission for CTC, at 500-nm excitation and at 535-nm emission for H_2DCFDA and, at 488-nm excitation and at 535-nm emission for BCECF, AM. Because of the evidence that the probe signal decays rapidly, images were captured within 5 minutes after the probe was added to pollen tubes. The procedures were repeated sequentially until 20 pollen tubes were displayed in each group for each experiment. In situ calibration of BCECF, AM was conducted according to Fricker et al. (1997) and the standard calibration curve representing the correlation between the ratiometric fluorescence and the pH of the samples was generated. For each treatment, images of different pollen samples were captured using same acquisition parameters and with one focal plane. For detailed image analysis, images were converted to 16 color scale using ImageJ. To analyze the quantitative localization of Ca^{2+}, ROS, and pH within the pollen tube, normalized fluorescence intensity analysis was performed on 20 pollen tubes with equivalent length for each group. To assess accumulation at the apex, normalized fluorescence intensities were measured in the area of the tube covering the first 10 µm from the apex using the "Rectangle Selection" tool of ImageJ. Signals have been reset against the background noise. The regions of interest (ROI) are shown on the figures. The fluorescence intensity measurement was also conducted inside the pollen tube along its growth axis, starting from the outermost tip to 50 µm backwards using the "Segmented Line" tool of ImageJ with a selection width of about 4 µm. Segments are shown on the figures. Based on the average of 20 measurement results, representative graphics were created by ImageJ.

2.5. Analysis of data

Three technical replicates were conducted for each experiment in each group. Statistical analyses were performed by SPSS 16.0 software, and data were subjected to one-way analysis of variance (ANOVA) with a threshold P value of 0.05.

3. Results

The germination rate and pollen tube length were first measured to find out the effects of Spd treatment, of cold stress, and of Spd treatment concomitantly with cold stress. Pollen germination rate increased after Spd treatments, with stimulation by 24% at 0.05 mM and by 14% at 0.1 mM compared with the control (Fig. 1a). In addition, pollen tube length rate increased after Spd treatments, with stimulation by 19% at 0.05 mM and by 8% at 0.1 mM compared with the control (Fig. 1b). The significant increase in germination rate and pollen tube length was only detected at 0.05 mM and 0.1 mM Spd treatments. As expected, the germination rate and pollen tube length were significantly decreased after cold stress by 10% and 16%, respectively (Fig. 1a, b). After detecting the stimulating effects of Spd treatments and the negative effects of cold stress, the concomitant effect of Spd treatment and cold stress was investigated. According to results, Spd treatment concomitantly with cold stress again stimulated the pollen germination rates and pollen tube length. Pollen germination rate was increased by 10% at 0.05 mM as compared with the cold stress case (Fig. 1a). Pollen tube length significantly increased by 8% at 0.025 mM, 19% at 0.05 mM and 10% at 0.1 mM when compared with cold stressed-pollen tubes (Fig. 1b). However, most stimulating effect was found at 0.05 mM. Therefore, it was concluded that cold-induced decrease in pollen germination rate and pollen tube growth could be alleviated by concomitant 0.05 mM spermidine treatment. Only four groups were examined in the next experiments: control, 0.05 mM Spd-treated, cold stress-treated and 0.05 mM Spd/cold stress-treated pollen tubes.

To investigate the effects of Spd treatment, cold stress, and Spd + cold stress treatment on pollen tube morphology, the abnormality rate of pollen tubes was analyzed. Node formation, curling, fluctuation of tube and swelling of the tube apex was considered as tube abnormality. Although some minor anomalies could be observed in the control group, pollen tubes generally showed a regular morphology, namely a cylindrical shape with an apical dome (Fig. 2a). After Spd treatment, the tube abnormality rate did not change significantly in comparison to control, although some minor anomalies such as swollen apex were visible (Fig. 2a, b). However, cold stress significantly stimulated abnormal pollen tube formation. The rate of pollen tube abnormalities significantly increased by 121%, in comparison to control (Fig. 2b). The most common abnormalities were extreme swelling of tube apex and node formation (Fig. 2a). Interestingly, it was found that the tube abnormality rate was attenuated when Spd was applied simultaneously with cold stress. Although the abnormality rate significantly decreased by 54% when compared to cold stress, some abnormalities were still observable (Fig. 2b), with the most common abnormalities being curling and swelling of tube apex (Fig. 2a).

Because the proper organization of the actin cytoskeleton is required for pollen tube elongation, the distribution of actin filaments was examined. Actin filaments were observed as small and randomly-oriented in the tube apex while they turned as parallel filaments in the shank of controls and Spd-treated pollen tubes (Fig. 2c, d). However, the organization of actin filaments changed under cold stress conditions. Actin filaments in the shank did not appear as fibrillary structures. In addition, actin filaments seemed to be more densely packed in the expanded regions of pollen tubes while, on the contrary, they appeared as dispersed in the other regions (Fig. 2e).

After treatment with Spd in conjunction with cold stress, some effects or disorders in the organization of actin filaments were still observed; however, these symptoms were not as evident as in the cold stress group. While actin filaments were oriented as parallel in the tube shank (like in control and in Spd-supplemented tubes), actin filaments at the apex seemed indeed disorganized and dispersed but not as much as in the cold-stressed tubes (Fig. 2f). Anisotropy values of actin filaments were computed to determine the differences in the apex and shank between the groups. After Spd treatment, anisotropy of actin filaments in the apex significantly decreased by 38% in comparison with the control. After cold stress, anisotropy of actin filaments in the apex significantly increased by 148% in comparison with the control. When Spd was applied simultaneously with cold stress, the aberrant changes in anisotropy level of actin filaments caused by cold stress were ameliorated. In fact, no significant differences occurred between the control and Spd-treated pollen tubes under cold stress; nevertheless, anisotropy significantly decreased by 54% in Spd/cold-treated pollen tubes in comparison with the cold stress case (Fig. 2g). In addition, after Spd treatment, anisotropy of actin filaments in the shank significantly decreased by 20% in comparison with the control. After cold stress, anisotropy of actin filaments in the shank significantly increased by 32% in comparison with the control. Nevertheless, anisotropy of actin filaments in the shank decreased meaningfully by 14% in Spd/cold-treated pollen tubes in comparison with the cold stress group (Fig. 2h). These data indicate quite clearly that addition of Spd in conjunction with cold stress is able to reverse the disorganization of actin filaments induced by cold stress alone.

Since changes in the actin filament organization affect the proper transport of newly synthesized cell wall materials to the tube tip, the cell wall structure of pollen tubes was examined. In controls, Calcofluor White-labelled cellulose was present in the pollen tube cell wall, including the apex (Fig. 3a). After addition of Spd, cold stress and application of Spd concomitantly with cold stress, we found no differences in cellulose distribution in the apex and shank regions between the treatments (Fig. 3b, c, d). To reveal the detailed difference of cellulose distribution, normalized fluorescence intensities of Calcofluor White were computed in the area corresponding to the first 10 μm from the apex. We therefore focused on a fairly restricted area corresponding to the growth zone where most of the secretory vesicles fuse; this allowed us to obtain information on the production of cellulose in the area of highest vesicular secretion. According to results, intensity at the tip did not show notable changes between treatments (Fig. 3e). Cellulose distribution throughout the pollen tube cell wall was also investigated on the cell border from the tube apex down to 50 μm. In control pollen tubes, cellulose deposition was found to rapidly accumulate up to 10 μm, then showed a relatively even distribution after 10 μm. After Spd treatment, cellulose showed a relatively even distribution throughout the pollen tube. The graph of Spd was similar to the control case, particularly where the hemispherical curvature of the tube ends. In the cold-stressed group, cellulose showed a relatively even distribution in the first 20 μm; however, it showed a more irregular distribution afterwards. After Spd treatment under cold stress, cellulose exhibited a relatively even distribution between 0-6 μm while exhibiting a more irregular distribution afterwards (Fig. 3f). Although measurements of fluorescence intensity apparently indicated fluctuations in cellulose levels, they were all within the same range, suggesting that cellulose distribution did not differ substantially in the various cases analyzed.

Callose deposition, as shown by Aniline-Blue staining, was observed in the cell wall of pollen tubes of control samples except in the apex (Fig. 4a). After Spd treatment, callose accumulation did not show significant difference when compared with the control (Fig. 4b). However, dense callose accumulation was found throughout

the pollen tube cell wall in the cold stressed group, especially at the apex (Fig 4c). After Spd treatment concomitantly with cold stress, callose accumulation at the apex was still visible (Fig. 4d). For more in-depth analysis, normalized fluorescence intensities of Aniline Blue were computed in the area corresponding to the first 10 μm of each apex. As in the case of cellulose, measuring the normalized fluorescence intensity in a fairly narrow area of the apex allowed us to focus in the region of highest vesicular secretion. In this case, the normalized fluorescence intensity increased significantly by 82% after cold stress compared to the control group. However, the normalized fluorescence intensity decreased by 17% after treatment with Spd in conjunction with cold stress when compared to the group under cold stress only (Fig. 4e). Callose distribution throughout the pollen tube cell wall was also investigated on the cell border from the apex down to 50 μm. In the control group, callose was found to be at very low level at the apex and to increase after 30 μm. After treatment with Spd, callose was still at low level at the apex but it increased in intensity after about 20 μm. In the cold stressed group, callose accumulated quite intensively and rapidly up to 10 μm while exhibiting an uneven distribution between 10-50 μm. In these conditions, callose levels seemed to fluctuate as if its deposition was somehow disturbed. After Spd treatment under cold stress, callose exhibited a relatively low accumulation between 0-10 μm but increased rapidly and constantly afterwards. Briefly, while cold treatment resulted in an albeit oscillating leveling of callose content in the cell wall, the simultaneous application of Spd had the effect of decreasing the callose content at the apex and contrasting subsequent callose oscillations (Fig. 4f).

We examined the content of Ca^{2+} in the organelle/vesicle-rich area near the apex because its proper distribution is fundamental for a regular growth of pollen tubes. In control pollen tubes, the Ca^{2+} signal was intense at the apex while it gradually attenuated towards the distal part. This distribution is an indication of the Ca^{2+}-gradient that is necessary for pollen tubes to elongate (Fig. 5a). Ca^{2+} signal at the tube apex slightly decreased after Spd treatment (Fig 5b). After cold stress, Ca^{2+} signal increased at the tube apex (Fig. 5c), while, after Spd treatment plus cold stress, the apparent Ca^{2+} concentration at the apex was relatively high, but the Ca^{2+}-gradient throughout the pollen tube was much more appreciable than in the cold stress group (Fig. 5d). To analyze the detailed difference of Ca^{2+} signal in the apex, normalized fluorescence intensity was computed in the area that covers the first 10 μm of each apex. Ca^{2+} signal decreased by 33% after Spd treatment and increased by 23% after cold stress when compared to the control. After Spd treatment under cold stress Ca^{2+} signal decreased by 11% when compared to cold stress (Fig. 5e). To analyze the differences of Ca^{2+}-gradient, the fluorescence signals throughout the tube from the apex down to 50 μm were determined. In the control group, the Ca^{2+} signal at the tube tip increased intermittently up to 20 μm, decreased between 20-26 μm. Although Ca^{2+} signal exhibited a relatively regular distribution between 26-38 μm, it decreased after 38 μm. After Spd treatment, the Ca^{2+} signal at the tube tip increased up to 10 μm, decreased between 10-20 μm and showed a relatively regular distribution between 20-50 μm. However, in the cold stress group the Ca^{2+} signal in the apex was high and rapidly decreased after 24 μm. After Spd treatment under cold stress, the Ca^{2+} signal in the apex was still high but is more restricted than cold stress, although not yet comparable to control (Fig. 5e).

As cold stress affected Ca^{2+} distribution, and concomitant application of Spd attenuated the effect of cold stress, we next determined if cold stress and Spd/cold stress changed the distribution of ROS in the pollen tube. In the control and Spd-treated group, the ROS fluorescence signal was detected evenly throughout the pollen tube (Fig. 6a, b) although the control apparently showed a slight accumulation of ROS at the tube apex. However, it

was found that the ROS signal was much more intense in the tube apex after cold stress (Fig. 6c). Although the ROS signal was again very intense in the tube apex after Spd + cold stress treatment, the ROS concentration in the apex was not as prominent as in the cold stress group; nevertheless, it was higher than in both control and Spd-treated pollen tubes (Fig. 6d). To appreciate more the difference of apex-localized ROS fluorescence signal, the normalized fluorescence intensity was computed in the area that covers the first 10 µm of each apex. Again, we focused on a very narrow area at the tip corresponding to the highest vesicular secretion area. ROS fluorescence signal was significantly decreased by 37% after Spd treatment and significantly increased by 93% after cold stress when compared to the control. ROS fluorescence signal was significantly decreased by 53% after concomitant applications of cold stress and Spd in comparison to the cold stress group (Fig. 6e). To analyze the differences of ROS accumulation, fluorescence signals throughout the tube from the apex down to 50 µm were determined. In the control group, ROS were evenly distributed along the tube. After Spd treatment, low ROS level increased up to 20 µm and exhibited almost equivalent accumulation along the tube after 20 µm. In the cold stressed group, ROS signal significantly increased between 0 µm and 20 µm from the tip, while it decreased afterwards. In the Spd/cold stress group, the ROS signal increased again between 0-10 µm, but rapidly decreased soon after and exhibited an almost even accumulation along the rest of pollen tube (Fig. 6f).

As changes in pH also affect the growth of tip elongating cells, pH of pollen tubes was analyzed. In the control and Spd treated pollen tubes, the pH appeared as a gradient with more acidic values at the tube apex but progressively increasing towards the shank (Fig. 7a, b). However, after cold stress, acidification of the cytosol at the apex was quite evident and the acidic pH region extended backward (Fig. 7c). When cold stressed-pollen tubes were also incubated with Spd, the region with more acidic pH again refocused at the tip; although it was not comparable to control samples, the acidic pH region was more restricted in comparison to the cold stress group (Fig. 7d). To analyze the detailed difference of acidic pH signal in the apex, normalized fluorescence intensity of BCEF-AM was computed in the area that covers the first 10 µm of each apex. Although acidity did not show significant difference after Spd treatment, acidity was significantly increased by 58% after cold stress when compared to the control. However, Spd treatment under cold stress significantly decreased the acidity by 55%, in comparison to cold stress (Fig. 7e). To analyze the differences in acidity in pollen tubes, we measured the fluorescence signals throughout the tube, starting from the most extreme tip up to 50 µm back. In the control group, acidity is high at the apex but decreases after about 10 µm. After treatment with Spd, acidity at the tube tip is less focused and tends to decrease only after about 20 µm. In the group of cold treated pollen tubes, acidity is very intense and extended evenly backwards suggesting that the acidification of cytoplasm affects both the apical and subapical area. In the group treated with both Spd and cold stress, the acid region is still relatively large but is more restricted than cold stress, although not yet comparable to control. (Fig. 7f).

4. Discussion

Reproductive process, especially pollen development, germination, and tube elongation, are highly vulnerable to cold stress (Parrotta et al., 2019; Sorkheh et al., 2018). Harmful effects of cold stress on pollen tubes were determined in many species, including tea. For instance, pollen germination rate and pollen tube length were significantly hampered by cold stress in *Pyrus bretschneideri* (Gao et al., 2014), in *Pyrus pyrifolia* (Wu et al., 2012) and in four *Corylus avellana* genotypes (Çetinbaş-Genç et al., 2019a). Wang et al. (2016) suggested that low temperature treatment reduced the tube length more than 2 folds in *Camellia sinensis*. By analogy with these

studies, we found that cold stress significantly reduced both pollen germination rate and tube length, again confirming that cold stress can have severe repercussions on the fertilization process of plants.

Relevant doses of PA can have a stimulating effect on pollen germination and tube elongation (Wolukau et al., 2004; Sorkheh et al., 2011). For instance, it was reported that exogenously supplied Spd at 0.01 and 0.05 mM concentration had a stimulating effect on pollen germination and tube growth while exogenously supplied Spd at 0.25, 0.5 and 2.5 mM concentration had inhibitory effects in *Prunus mume* pollen tubes (Wolukau et al., 2004). In this study, exogenously supplied Spd at 0.05 mM and 0.1 mM concentration were found to significantly improve pollen germination and tube growth. However, the most stimulating effect was found at 0.05 mM. That the stimulating effect of Spd is related to its dose is not surprising because the effect of exogenous PA on cells may vary depending on the type and dose of PA, in addition to the processed plant species (Aloisi et al., 2016a). It was shown that exogenously supplied Spd at 0.01 mM and 0.05 mM concentration increased pollen germination rate in *Nicotiana tabacum* while the most stimulating effect was determined at 0.01 mM (Benko et al., 2019). It is also known that plant growth regulators, including PA, can improve pollen tube growth under various stressful conditions in strawberry (Voyiatzsis et al., 2005). Wolukau et al. (2004) reported that 0.005 mM and 0.025 mM Spd treatments increased the pollen germination rate under cold stress, and 0.005 mM Spd treatment also increased pollen tube length under cold stress in *Prunus mume*. According to our results, Spd treatment stimulated the pollen germination rate and pollen tube length under cold stress and the most stimulating effect was determined at 0.05 mM Spd.

Various stresses cause changes in the tube morphology, especially at the tube apex (the most sensitive area). For instance, tube abnormalities have been reported as induced by phenylboronic acid in *Malus domestica* (Fang et al., 2016), by quizalofop-P-ethyl in *Hyacinthus orientalis* (Deveci et al., 2017) and by aminolevunic acid in *Pyrus pyrifolia* (An et al., 2018). It has been reported that even cold stress conditions can induce tube abnormalities. For instance, cold stress induced tube swelling in *Nicotiana tabacum* (Parrotta et al., 2019) and in *Corylus avellana* (Çetinbaş-Genç et al., 2019a). According to our results, cold stress significantly increased the tube abnormalities (such as swelling, node formation and curling) approximately 2-fold when compared to the control. Wang et al. (2016) have previously reported similar increase rates of tube abnormalities in *Camellia sinensis* cold-treated pollen tubes. Besides various stresses, it has been known that PA treatment can change tube morphology. For instance, various abnormalities were observed in *Pyrus communis* (Aloisi et al., 2015) after Spm treatment, in *Camellia sinensis* after Put treatment (Çetinbaş-Genç, 2019) and in *Corylus avellana* after Put treatment (Çetinbaş-Genç et al., 2019b). In our case study, cold stress induces profound changes in the morphology of pollen tubes; on the contrary, treatment with Spd does not produce any particular effects, indeed Spd has the ability to significantly reduce the rate of morphological abnormalities caused by cold. Therefore, Spd, when applied to the appropriate dosage, can counteract the negative effects of cold helping to rebalance the growth process of pollen tubes.

The morphology of pollen tubes is the result of a complex series of cellular events, from ion flux to the correct deposition of cell wall polysaccharides, through the correct organization of the cytoskeleton. Proper organization and dynamics of the actin cytoskeleton are requisite for the proper elongation and functionality of the pollen tube (Cai et al., 2015). Changes in the actin cytoskeleton orientation may lead to modifications of tube morphology and alteration of several biochemical processes (Qu et al., 2015). Actin filaments, in cooperation with

other processes such as ion flux, are effectively responsible for focusing the fusion of secretory vesicles in a restricted area, thus determining apical elongation and maintaining the cylindrical shape. When any stressful agent unbalances this process, it will cause secretory vesicles to fuse over a larger area of the plasma membrane, resulting in a swelling apex and incorrect growth. The actin cytoskeleton is known to be sensitive to various stresses (Kang et al. 2010) and in pollen tubes, it can be disrupted by various chemical treatments, as reported for different species (Wang et al., 2010; Ketelaar et al. 2012). Even during physiological stress such as that due to the self-incompatibility (SI) response, the organization of actin microfilaments is profoundly modified and self-pollen is induced to death. In fact, during the SI response, there is an abnormal aggregation of the microfilaments that could be favored by the enzymatic activity of transglutaminase which bind covalently PAs to glutamine residues of both actin and tubulin. In support of this, it is noted that PAs concentration increases significantly in soluble and insoluble perchloric acid fractions following the SI response. This is due at least in part to the binding catalyzed by transglutaminase whose activity definitely increases in the SI response: by binding PAs to proteins and / or peptides, TGase mediates some of the effects of PA (Del Duca et al., 2010). The actin cytoskeleton is also target of cold stress. Gao et al. (2015) reported that cold stress disrupted the actin cytoskeleton of pollen tubes leading to short pollen tubes in *Pyrus pyrifolia*. Besides, it has been shown that cold stress negatively affects the actin organization in pollen tubes of *Corylus avellana* cultivars (Çetinbaş-Genç, 2019a). In our case, the cold treatment of pollen tubes causes a profound change in the structure of actin filaments both in the tube shank and especially in the tube apex. These changes also reveal the cause of abnormalities in the tube apex after cold stress. According to our observations, cold stress-induced changes of actin structures were ameliorated by Spd treatment when concomitantly applied with cold stress, which is also confirmed by the anisotropy results. The increase in anisotropy of actin filaments after cold stress may explain the increase in morphological abnormalities as observed in pollen tubes (Cardenas et al., 2008; Ketelaar et al., 2012). The depolymerization of actin filaments at the apex may not be closely related to apex abnormalities. However, it should be noted that numerous works in the literature indicate that when actin filaments are depolymerized for causes other than cold, the apex very often changes shape and can expand due to a vesicular secretion that propagates over the entire apex surface (Cardenas et al., 2008; Ketelaar et al., 2012; Parrotta et al., 2019). The decrease in anisotropy as observed after Spd treatment can be interpreted as more dynamic actin structures (Boudaoud et al., 2014; Parrotta et al., 2016); in addition, highly dynamic actin filaments in the apex might be critical for pollen tubes to quickly adapt to new growing conditions (Cai et al., 2015). In cold-treated pollen tubes, anisotropy increases strikingly, thereby indicating a more random and perhaps less dynamic distribution of actin filaments. Although we do not have direct evidence, what is clear is that increasing anisotropy is also due to changes in the dynamics of actin filaments (Parrotta et al., 2016). This new configuration of apical actin may be responsible for morphological abnormalities. Compared to cold-treated pollen tubes, actin filament anisotropy in the shank does not decrease significantly, but actin anisotropy at the apex is close to control after that cold-stressed tubes are also treated with Spd. This indicates that actin filaments at the apex recover their dynamics after Spd treatment as opposed to pollen tubes inhibited only by cold. This situation explains the decrease of abnormality rate after Spd treatment concomitant with cold stress. Actin filaments are closely related to many other cellular components, such as the cell wall; in fact, it is along the actin filaments that newly synthesized cell wall materials are transported to the pollen tube apex (Cai et al., 2015). Actin filaments also control the distribution of both cellulose and callose synthase in the plasma membrane (Cai et al., 2011). Therefore, it is likely that alterations in the actin structure change both cellulose and callose accumulation in pollen

tubes (Cai et al., 2011; Chen et al., 2018). We found that cellulose distributed along the pollen tube cell wall in all groups analyzed, including the apex (Fang et al., 2016; Aloisi et al., 2017). However, differences in cellulose distribution were found after cold stress, especially in regions following the swollen apex. Interestingly, Spd treatment under cold stress reduced the accumulation of cellulose in that region. Similarly, Parrotta et al. (2019) have reported intense cellulose accumulation in *Nicotiana tabacum* pollen tube after cold stress, especially at the swollen apex. Similarly, intense cellulose accumulation at the swollen tube apex has been reported in Spm-treated tubes of *Pyrus communis* (Aloisi et al., 2017). These observations suggest that a higher deposition of cellulose at the apex of cold-stressed pollen tubes is part of the response that pollen tubes accomplish; hypothetically, a higher accumulation of cellulose could be used to counteract the swelling of the tube apex.

Callose is the most abundant component of the cell wall of pollen tubes, with the exception of the apex, and plays a more significant role than cellulose. Callose accumulation at the apex is considered an abnormal situation, generally related to dysfunctional or blocked pollen tubes, as occurs in SI response of *Pyrus communis* (Franklin-Tong et al., 1996; Del Duca et al., 2010). In control group, callose was located throughout the tube, except for the apex. However, higher callose accumulation at the apex was found after cold treatment. This might be probably related to the degradation of actin filaments and could explain the occurrence of short pollen tubes after cold stress. From the unfortunately few data in the literature, it is inferred that the synthesis of callose takes place due to callose synthase that is transported at the apex of pollen tubes most likely by secretory vesicles (Cai et al., 2011). Once present at the apex, callose synthase is most likely regulated by several conditions, also including its removal by endocytosis. However, this is currently only an unverified hypothesis. Therefore, assuming that actin filaments are more dynamic at the apex, this could not only imply an unbalanced secretion or insertion rate of callose synthase into the plasma membrane, but also an altered regulation of both its insertion sites and enzymatic activity. In addition, the data shown in this work indicate that the cold-induced depolymerization of actin filaments causes the pollen tube apex to expand. This means an unregulated secretion rate, i.e. in a wider area of the pollen tube apex, and could therefore imply that callose synthase is inserted in more points, thus resulting in disturbed callose production. The presence of callose at the tube apex could compromise tube growth more severely (Ünal et al., 2013). Dense callose accumulation at tube apex was also observed in pollen tubes of *Corylus avellana* after cold stress (Çetinbaş-Genç, 2019a). However, Parrotta et al. (2019) did not observed dense callose accumulation at the apex of *Nicotiana tabacum* pollen tubes after cold stress. Therefore, this might not be a general feature; it should be also considered that cold stress in *Nicotiana tabacum* was applied to ungerminated pollen grains while in our case cold stress was applied to germinating pollen. According to our results, callose deposition at the tube apex did not significantly decrease after Spd treatment of cold stressed-pollen tubes; this may indicate that, although Spd can rebalance some of the effects caused by cold stress, it fails to re-establish the correct synthesis of callose.

The growth of pollen tubes is the result of multiple, closely interconnected processes. The transport of polysaccharide and enzymatic components by secretory vesicles is the step by which new building blocks are added. However, the entire process has to be regulated and Ca^{2+} are one of the main regulatory agents. The CTC fluorescence probe labels the membrane bound Ca^{2+} (Kalra et al., 1999). We examined the Ca^{2+} content in the apex because this area is rich in organelles/vesicles allowing tube elongation; thus, the CTC fluorescence is associated to the organelle/vesicle-enriched area near the apex (Polito et al., 1983). We thought that changes in

membrane bound Ca^{2+} would be an indicator of organelle/vesicle activity and therefore of tube elongation. The strong CTC signal at the tube apex after cold treatment could also be related to the disorganization of actin filaments and therefore to an irregular transport of organelles/vesicles, while the decrease of the CTC signal after cold treatment + Spd could be due to the reorganization of actin filaments and the rebalancing of organelles/vesicles transport. Nor can it be excluded that the strong CTC signal at the tube apex after cold treatment is due to an altered membrane permeability (Saunders and Hepler et al, 1981). Hepler et al. (2016) reported that some stimuli may activate the Ca^{2+} permeable channels incorporated in the plasma membrane or endomembranes causing an alteration in membrane permeability. Thus Ca^{2+} can move down along the strong electrochemical gradient in the cytosol, leading to a rapid increase in $Ca^{2+.}$

The regulatory action of Ca^{2+} is exerted along with other molecules, such as ROS, considered among the most important substances in the control of pollen tube growth. The apex localized ROS modulates in turn the apical gradient of Ca^{2+} which can affect the organization of actin filaments and promote the correct growth of pollen tubes (Ren and Xiang, 2007; Potocky et al., 2007; Pasqualini et al., 2015; Domingos et al., 2015). The mechanism of ROS/Ca^{2+} crosstalk could also provide the tube with the opportunity to cope with stress. Changes in apex-localized ROS under stress conditions may modify the activity of Ca^{2+} channels located at the tube apex (Potocky et al., 2012; Kaya et al., 2014). The dissipation of Ca^{2+}-gradient and ROS accumulation at the apex after cold stress has already been reported (Wang et al., 2016; Parrotta et al., 2019). According to our results, Ca^{2+} is distributed over a larger apical area of the tube after cold stress (this may support the hypothesis of more widespread vesicular fusion). In addition, Ca^{2+} accumulation is more limited after Spd treatment of samples already subjected to cold stress. This evidence suggests that Spd is able to refocus the Ca^{2+} gradient in a narrower area. Similarly, Wang et al. (2016) and Parrotta et al. (2019) reported that the Ca^{2+} gradient dissipated after cold stress in pollen tubes of *Camellia sinensis* and *Nicotiana tabacum* respectively. Our results are in agreement with the literature suggesting that PA affects Ca^{2+} levels in *Camellia sinensis* pollen tubes. In addition, Ca^{2+} levels in pollen tubes can be modified by activating Ca^{2+} channels located in the plasma membrane (Pottosin et al., 2014). Therefore, it can be assumed that Spm may have affected Ca^{2+} levels by activating Ca^{2+} channels. According to the literature, it can be hypothesized that cold treatment causes an increase in Ca^{2+} levels at the tube apex, as triggered by increased Ca^{2+} channel activity or by their diffusion in a larger area. This hypothesis may also be related to the disorganization of actin filaments because the depolymerization of actin filaments may affect the apical Ca^{2+} gradient (Cardenas et al., 2008). Treatment with Spd, as reported in the literature (Pottosin et al., 2014), could rebalance ROS levels and thus buffer the Ca^{2+} ion content at the apex by acting on the plasma membrane channels.

Wang et al. (2016) and Parrotta et al. (2019) reported that cold stress increased the ROS signal in the tube apex of *Camellia sinensis* and *Nicotiana tabacum*, respectively. In agreement with those results, we observed that the apex-localized ROS accumulation increased approximately 3 times after cold stress. However, the content of ROS in the apex was reduced after Spd treatment of cold stressed-pollen tubes when compared with the cold stress case only. There is conflicting evidence on this issue. Wu et al. (2010) have reported that Spd increased the ROS level in pollen tubes of *Arabidopsis thaliana*, while Benko et al. (2019) stated that Spd decreased ROS levels in pollen tubes. Impaired Ca^{2+} gradient as observed after cold treatment could trigger an increase in ROS level at the tube apex (Potocky et al., 2012; Kaya et al., 2014); consequently, the altered $Ca2^{+}$ gradient would have important

effects on the organization of actin filaments (as well as on myosin activity). This would result in an altered movement of membranous structures along actin filaments thereby affecting the secretion of newly synthesized cell wall materials to the tube apex, and thus changing the composition of the pollen tube cell wall. This could explain both the presence of morphological aberrations and the occurrence of short pollen tubes after cold stress. It can be hypothesized that Spd ameliorates the cold-induced effects by scavenging ROS formation. Similarly, it has been reported that PA have an important role in the plant defense system by stimulating the antioxidant machinery and decreasing the oxidative stress intensity (Kubis, 2003; Aloisi et al., 2015;). Moreover, given that the most of cellular Spd pool is localized in the cell wall compartment (Bokern et al., 1995) and that PA interact with cell wall molecules, it is possible that phenolamides (a major group of secondary metabolites resulting from the conjugation of a phenolic moiety with PA) affect pollen germination by exerting a structural effect on the cell wall, which results more resistant. The study of the effects of cold stress on the cell wall and particularly the interaction of Spd with hydroxycynnamic acids deserves to be deepened.

The intracellular pH can also regulate various processes essential for pollen tube growth, although the relationship between H^+, Ca^{2+} and ROS is not yet clear. However, all three of these ions/molecules can interface with actin filaments (Felle, 1999). Previous works on *Lilium longiflorum* pollen tubes have shown slightly acidic pH in the apex and alkaline pH in the sub-apex (Feijo et al., 1999). Increase in the acidic pH leads to actin filament destabilization and inhibits pollen tube growth. In addition, ABPs are sensitive to pH changes (Lovy-Wheeler et al., 2005). Moreover, change in pH values within the pollen tube also lead to changes in apex-localized ROS accumulation. Wang et al. (2016) reported that cold stress induced the acidification of the pollen tube apex. Change in pH gradient in the pollen tube apex after cold stress was also found in *Nicotiana tabacum* (Parrotta et al., 2019). Consistent with these studies, we observed a significant increase in acidic pH in the tube apex after cold stress. We assume that increased acidity might interfere with the interaction between ABP and actin filaments, affecting vesicle secretion and thus leading to changes in cell wall properties. Moreover, we found that levels of acidic pH are partially restored after Spd treatment of cold stressed-pollen tubes, suggesting that PA can rebalance the pH homeostasis of pollen tubes.

After evaluating the results described in this work, we hypothesized an integration of data according to the scheme in Fig. 8. The actin cytoskeleton, the cell wall, Ca^{2+}, protons and ROS are only some of the factors involved in pollen tube growth and establishing their interconnection in case of cold stress and Spd treatment is not straightforward. Due to the many data already available in the literature, it is relatively easier to define possible connections between actin, Ca^{2+} and ROS. Basically, a proper dynamics of actin filaments generates a correct vesicular secretion process which results in an appropriate cell wall modelling; the latter allows the pollen tube to expand at the apex; the stretching of the apical plasma membrane causes an influx of Ca^{2+} ions which, boosted by the accumulation of ROS, contributes to the correct dynamics of actin filaments. Assuming that cold stress affects the dynamics of actin filaments , this would redistribute the vesicular secretion thereby altering the properties of the cell wall and reducing pollen tube growth because it expands over a larger surface area. A differential stretching of the apical plasma membrane alters the influx of Ca^{2+} ions and could result in an increase in ROS production. In the hypothesis that Spd restores the correct levels of ROS or acts directly on the Ca^{2+} channels, this would result in a partial recovery of the Ca^{2+} content; this could affect the dynamics of actin filaments and therefore the entire growth pathway of the pollen tube.

5. Conclusion

Cold stress-induced changes in pollen tubes can be partially alleviated by treatment of Spd in conjunction with cold stress. Spd treatment can reorganize the growth pattern of tubes, by modulating Ca^{+2} and ROS homeostasis, actin cytoskeleton organization, and cell wall deposition in *Camellia sinensis* pollen tube.

Author contributions

AÇG designed the study and performed experiments, analyzed data and wrote the manuscript. GC and SDD analyzed data, provided vital advice and wrote the manuscript. All authors approved the manuscript.

Conflicts of interest

We declared we have no conflict of interest that that represents a conflict of interest in connection with the work submitted.

Acknowledgements

This research did not receive any specific grant from funding agencies in the public, commercial, or not-for-profit sectors.

References

Aloisi, I., Cai, G., Faleri, C., Navazio, L., Serafini-Fracassini, D., Del Duca, S., 2017. Spermine regulates pollen tube growth by modulating Ca^{2+}- dependent actin organization and cell wall structure. Front. Plant Sci. 8, 1701.

Aloisi, I., Cai, G., Serafini-Fracassini, D., Del Duca, S., 2016a. Polyamines in pollen: from microsporogenesis to fertilization. Front. Plant Sci. 7, 155.

Aloisi, I., Cai, G., Serafini-Fracassini, D., Del Duca, S., 2016b. Transglutaminase as polyamine mediator in plant growth and differentiation. Amino Acids 48, 2467-2478.

Aloisi, I., Cai, G., Tumiatti, V., Minarini, A., Del Duca, S., 2015. Natural polyamines and synthetic analogs modify the growth and the morphology of Pyrus communis pollen tubes affecting ROS levels and causing cell death. Plant Sci. 239, 92–105.

Alvarez, I., Tomaro, M.L., Benavides, M.P., 2003. Changes in polyamines, proline and ethylene in sunflower calluses treated with NaCl. Plant Cell Tiss. Org. 74, 51-59.

An, Y.Y., Lu, W.Y., Li, J., Wang, L.J., 2018. ALA inhibits pear pollen tube growth through regulation of vesicle trafficking. Sci. Hortic. 241, 41-50.

Benko, P., Jee, S., Kaszler, N., Feher, A., Gemes, K., 2019. Polyamines treatment during pollen germination and pollen tube elongation in tobacco modulate reactive oxygen species and nitric oxide homeostasis. J. Plant Physiol. 244, 153085.

Bokern, M., Witte, L., Wray, V., Nimtz, M., Meurer-Grimes, B., 1995. Trisubstituted hydroxycinnamic acid spermidines from Quercus dentata pollen. Phytochemistry 39, 1371-1375.

Bora, K., Sarkar, D., Konwar, K., Payeng, B., Sood, K., Paul, R.K., Datta, R., Das, S., Khare, P., Karak, T., 2019. Disentanglement of the secrets of aluminium in acidophilic tea plant (Camellia sinensis L.) influenced by organic and inorganic amendments. Food Res. Int. 120, 851-864.

Boudaoud, A., Burian, A., Borowska-Wykret, D., Uyttewaal, M., Wrzalik, R., Kwiatkowska, D., Hamant, O., 2014. FibrilTool, an ImageJ plug-in to quantify fibrillar structures in raw microscopy images. Nat. Protoc. 9, 457-463.

Brewbaker, J.L., Kwack, B.H., 1963. The essential role of calcium ion in pollen germination and pollen tube growth. Am. J. Bot. 50, 859– 865.

Cai, G., Cresti, M., 2010. Microtubule motors and pollen tube growth—still an open question. Protoplasma 247, 131–143.

Cai, G., Faleri, C., Del Casino, C., Emons, A.M.C, Cresti, M., 2011. Distribution of callose synthase, cellulose synthase, and sucrose synthase in tobacco pollen tube is controlled in dissimilar ways by actin filaments and microtubules. Plant Physiol. 155, 1169–1190.

Cai, G., Parrotta, L., Cresti, M., 2015. Organelle trafficking, the cytoskeleton, and pollen tube growth. J. Integr. Plant Biol. 57, 63–78.

Cardenas, L., Lovy-Wheeler, A., Kunkel, J.G., Hepler, P.K., 2008. Pollen tube growth oscillations and intracellular calcium levels are reversibly modulated by actin polymerization. Plant Physiol. 146, 1611-1621.

Çetin, E., Yildirim, C., Palavan-Ünsal, N., Ünal, M., 2000. Effect of spermine and cyclohexylamine on in vitro pollen germination and tube growth in Helianthus annuus. Can. J. Plant Sci. 80, 241–245.

Çetinbaş-Genç, A., 2019. Putrescine modifies the pollen tube growth of tea (Camellia sinensis) by affecting actin organization and cell wall structure. Protoplasma 257, 89-101.

Çetinbaş-Genç, A., Cai, G., Del Duca, S., Vardar, F., Ünal, M., 2019b. The effect of putrescine on pollen performance in hazelnut (Corylus avellana L.). Sci. Hortic. 261, 108971.

Çetinbaş-Genç, A., Cai, G., Vardar, F., Ünal, M., 2019a. Differential effects of low and high temperature stress on pollen germination and tube length of hazelnut (Corylus avellana L.) genotypes. Sci. Hortic. 255, 61-69.

Charnay, D., Nari, J., Norat, G., 1992. Regulation of plant cell-wall pectin methyl esterase by polyamines-interactions with the effects of metal ions. Eur. J. Biochem. 205, 711–714.

Chen, J., Wang, P., de Graaf, B.H., Zhang, H., Jiao, H., Tang, C., Zhang, S., Wu, J., 2018. Phosphatidic acid counteracts S-RNase signaling in pollen by stabilizing the actin cytoskeleton. Plant Cell 30,1023–1039.

Chen, T., Teng, N., Wu, X., Wang, Y., Tang, W., Samaj, J., Baluska, F., Lin, J., 2007. Disruption of actin filaments by latrunculin B affects cell wall construction in Picea meyeri pollen tube by disturbing vesicle trafficking. Plant Cell Physiol. 48, 19–30.

Del Duca, S., Cai, G., Di Sandro, A., Serafini-Fracassini, D., 2010. Compatible and self-incompatible pollination in Pyrus communis displays different polyamine levels and transglutaminase activity. Amino Acids, 38, 659-667.

Del Duca, S., Serafini-Fracassini, D., Bonner, P.L.R., Cresti, M., Cai, G., 2009. Effects of post-translational modifications catalyzed by pollen transglutaminase on the functional properties of microtubules and actin filaments. Biochem. J. 418, 651–664.

Deveci, A., Aksoy, O., Al, G., 2017. Investigation of the effects of quizalofop-P-ethyl on pollen germination of Hyacinthus orientalis L.. Caryologia 70, 77–81.

Dixin, C., Shaoling, Z., 2002. Effects of polyamines and polyamine synthesis inhibitor on in vitro pollen germination and tube growth in pears. Journal of Fruit Science 19, 377-380.

Doblin, M.S., De Melis, L., Newbigin, E., Bacic, A., Read, S.M., 2001. Pollen tubes of Nicotiana alata express two genes from different β-glucan synthase families. Plant Physiol. 125, 2040-2052.

Domingos, P., Prado, A.M., Wong, A., Gehring, C., Feijo, J.A., 2015. Nitric oxide: a multitasked signaling gas in plants. Mol. Plant 8, 506–520.

Elejalde-Palmett, C., de Bernonville, T.D., Glevarec, G., Pichon, O., Papon, N., Courdavault, V., St-Pierre, B., Giglioli-Guivarc'h, N., Lanoue, A., Besseau, S., 2015. Characterization of a spermidine hydroxycinnamoyltransferase in Malus domestica highlights the evolutionary conservation of trihydroxycinnamoyl spermidines in pollen coat of core Eudicotyledons. J. Exp. Bot. 66, 7271-7285.

Erland, L.A.E., Mahmoud, S.S., 2014. An efficient method for regeneration of lavandin (Lavandula x intermedia cv. 'Grosso'). In Vitro Cell. Dev. Biol. Plant 50, 646–654.

Fang, K., Zhang, W., Xing, Y., Zhang, Q., Yang, L., Cao, Q., Qin, L., 2016. Boron toxicity causes multiple effects on Malus domestica pollen tube growth. Front. Plant Sci. 7, 208.

Feijo, J.A., Sainhas, J., Hackett, G.R., Kunkel, J.G., Hepler, P.K., 1999. Growing pollen tubes possess a constituitive alkaline band in the clear zone and a growth-dependent acidic tip. J. Cell Biol. 144, 483–496.

Felle, H.H., 2001. pH: signal and messenger in plant cells. Plant Biol. 3, 577-591.

Franklin-Tong, V.E., Drobak, B.K., Allan, A.C., Watkins, P.A., Trewavas, A.J., 1996. Growth of pollen tubes of Papaver rhoeas is regulated by a slow-moving calcium wave propagated by inositol 1, 4, 5-trisphosphate. The Plant Cell 8,1305-1321.

Fricker, M.D., White, N.S., Obermeyer, G., 1997. pH gradients are not associated with tip growth in pollen tubes of Lilium longiflorum. J. Cell Sci. 110, 1729-1740.

Gao, Y., Zhou, H., Chen, J., Jiang, X., Tao, S., Wu, J., Zhang, S., 2015. Mitochondrial dysfunction mediated by cytoplasmic acidification results in pollen tube growth cessation in Pyrus pyrifolia. Physiol. Plant. 153, 603-615.

Gao, Y.B., Wang, C.L., Wu, J.Y., Zhou, H.S., Jiang, X.T., Wu, J., Zhang, S.L., 2014. Low temperature inhibits pollen tube growth by disruption of both tip-localized reactive oxygen species and endocytosis in Pyrus bretschneideri Rehd. Plant Physiol. Bioch. 74, 255-262.

Goubet, F., Misrahi, A., Park, S. K., Zhang, Z., Twell, D., Dupree, P., 2003. AtCSLA7, a cellulose synthase-like putative glycosyltransferase, is important for pollen tube growth and embryogenesis in Arabidopsis. Plant Physiol. 131, 547-557.

Grienenberger, E., Besseau, S., Geoffroy, P., Debayle, D., Heintz, D., Lapierre, C., Pollet, B., Heitz, T., Legrand, M., 2009. A BAHD acyltransferase is expressed in the tapetum of Arabidopsis anthers and is involved in the synthesis of hydroxycinnamoyl spermidines. Plant J. 58, 246-259.

Haq, S., Boz, I., 2018. Developing a set of indicators to measure sustainability of tea cultivating farms in Rize Province, Turkey. Ecol. Indic. 95, 219-232.

Hebbar, K.B., Rose, H.M., Nair, A.R., Kannan, S., Niral, V., Arivalagan M., Gupta, M.A., Samsudeen, K., Chandran, K.P., Chowdappa, P., Prasad, P.V., 2018. Differences in in vitro pollen germination and pollen

tube growth of coconut (Cocos nucifera L.) cultivars in response to high temperature stress. Environ. Exp. Bot. 153, 35-44.

Hedhly, A., Hormaza, J.I., Herrero, M., 2005. The effect of temperature on pollen germination, pollen tube growth, and stigmatic receptivity in peach. Plant Biol. 7, 476-483.

Holdaway-Clarke, T.L., Hepler, P.K, 2003. Control of pollen tube growth: role of ion gradients and fluxes. New Phytologist 159, 539-563.

Kalra, G., Bhatla, S.C., 1999. Distribution of membrane-bound calcium and activated calmodulin in cultured protoplasts of sunflower (Helianthus annuus L.). Curr Sci. 76, 1580-1584.

Kang, S., Chen, S., Dai, S., 2010. Proteomics characteristics of rice leaves in response to environmental factors. Front. Biol. 5, 246–254.

Kaya, H., Nakajima, R., Iwano, M., Kanaoka, M.M., Kimura, S., Takeda, S., Kawarazaki, T., Senzaki, E., Hamamura, Y., Higashiyama, T., Takayama, S., Abe, M., Kuchitsu, K., 2014. Ca2+-activated reactive oxygen species production by Arabidopsis RbohH andRbohJ is essential for proper pollen tube tip growth. Plant Cell, 26, 1069–1080.

Ketelaar, T., Meijer, H.J., Spiekerman, M., Weide, R., Govers, F., 2012. Effects of latrunculin B on the actin cytoskeleton and hyphal growth in Phytophthora infestans. Fungal Genet. Biol. 49, 1014-1022.

Kubis, J., 2003. Polyamines and" scavenging system": influence of exogenous spermidine on catalase and guaiacol peroxidase activities, and free polyamine level in barley leaves under water deficit. Acta Physiol. Plant. 25, 337-343.

Lassig, R., Gutermuth, T., Bey, T. D., Konrad, K. R., Romeis, T., 2014. Pollen tube NAD(P)H oxidases act as a speed control to dampen growth rate oscillations during polarized cell growth. Plant Journal 78, 94-106.

Lazzaro, M.D., Donohue, J.M., Soodavar, F.M., 2003. Disruption of cellulose synthesis by isoxaben causes tip swelling and disorganizes cortical microtubules in elongating conifer pollen tubes. Protoplasma 220, 201–207.

Li, H., Bacic, A., Read, S. M., 1997. Activation of pollen tube callose synthase by detergents (evidence for different mechanisms of action). Plant Physiol. 114, 1255-1265.

Li, J., Arkorful, E., Cheng, S., Zhou, Q., Li, H., Chen, X., Sun, K., Li, X., 2018. Alleviation of cold damage by exogenous application of melatonin in vegetatively propagated tea plant (Camellia sinensis (L.) O. Kuntze). Sci. Hortic. 238, 356-362.

Lovy-Wheeler, A., Wilsen, K.L., Baskin, T.I., Hepler, P.K., 2005. Enhanced fixation reveals the apical cortical fringe of actin filaments as a consistent feature of the pollen tube. Planta 221, 95–104.

Malho, R., Camacho, L., Moutinho, A., 2000. Signalling pathways in pollen tube growth and reorientation. Ann. Bot. 85, 59-68.

McCurdy, D.W., 1999. Rapid communication: Is 2,3-butanedione monoxime an effective inhibitor of myosin-based activities in plant cells. Protoplasma 209, 120-125.

Pan, J., Wang, W., Li, D., Shu, Z., Ye, X., Chang, P., Wang, Y., 2016. Gene expression profile indicates involvement of NO in Camellia sinensis pollen tube growth at low temperature. BMC Genomics 17, 809.

Parrotta, L., Faleri, C., Cresti, M., Cai, G., 2016. Heat stress affects the cytoskeleton and the delivery of sucrose synthase in tobacco pollen tubes. Planta 243, 43–63.

Parrotta, L., Faleri, C., Guerriero, G., Cai, G., 2019. Cold stress affects cell wall deposition and growth pattern in tobacco pollen tubes. Plant Sci. 283, 329–342.

Pascoa, R.N., Teixeira, A.M., Sousa, C., 2019. Antioxidant capacity of Camellia japonica cultivars assessed by near-and mid-infrared spectroscopy. Planta 249,1053-1062.

Pasqualini, S., Cresti, M., Del Casino, C., Faleri, C., Frenguelli, G., Tedeschini, E., Ederli, L., 2015. Roles for NO and ROS signalling in pollen germination and pollen-tube elongation in Cupressus arizonica. Biol. Plant 59, 735–744.

Persia, D., Cai, G., Del Casino, C., Faleri, C., Willemse, M.T., Cresti, M., 2008. Sucrose synthase is associated with the cell wall of tobacco pollen tubes. Plant Physiol. 147, 1603–1618.

Pham, V.T., Herrero, M., Hormaza, J.I., 2015. Effect of temperature on pollen germination and pollen tube growth in longan (Dimocarpus longan Lour.). Sci. Hortic. 197, 470-475.

Polito, V.S., 1983. Membrane-associated calcium during pollen grain germination: a microfluorometric analysis. Protoplasma 117, 226-232.

Potocky, M., Jones, M.A., Bezvoda, R., Smirnoff, N., Zarsky, V., 2007. Reactive oxygen species produced by NADPH oxidase are involved in pollen tube growth. New Phytol. 174, 742–751.

Potocky, M., Pejchar, P., Gutkowska, M., Jimenez-Quesada, M.J., Potocka, A., de Dios Alche, J., Kost, B., Zarsky, V., 2012. NADPH oxidase activity in pollen tubes is affected by calcium ions, signaling phospholipids and Rac/Rop GTPases. J. Plant Physiol. 169, 1654–1663.

Pottosin, I., Shabala, S., 2014. Polyamines control of cation transport across plant membranes: implications for ion homeostasis and abiotic stress signaling. Front. Plant Sci. 5, 154.

Qu, X., Jiang, Y., Chang, M., Liu, X., Zhang, R., Huang, S., 2015. Organization and regulation of the actin cytoskeleton in the pollen tube. Front. Plant Sci. 5, 786.

Ren, H., Xiang, Y., 2007. The function of actin-binding proteins in pollen tube growth. Protoplasma 230, 171-182.

Sagor, G.H.M., Berberich, T., Takahashi, Y., Niitsu, M., Kusano, T., 2013. The polyamine spermine protects Arabidopsis from heat stress-induced damage by increasing expression of heat shock-related genes. Transgenic Res. 22, 595-605.

Saunders, M. J., Hepler, P. K., 1981. Localization of membrane-associated calcium following cytokinin treatment in Funaria using chlorotetracycline. Planta 152, 272-281.

Sequera-Mutiozabal, M., Antoniou, C., Tiburcio, A.F., Alcazar, R., Fotopoulos, V., 2017. Polyamines: emerging hubs promoting drought and salt stress tolerance in plants. Curr. Mol. Biol. Rep. 3, 28–36.

Serrazina, S., Dias, F.V., Malho, R., 2014. Characterization of FAB 1 phosphatidylinositol kinases in Arabidopsis pollen tube growth and fertilization. New Phytol. 203, 784-793.

Song, J., Nada, K., Tachibana, S., 1999. Ameliorative effect of polyamines on the high temperature inhibition of in vitro pollen germination in tomato (Lycopersicon esculentum Mill.). Sci. Hortic. 80, 203-212.

Sorkheh, K., Azimkhani, R., Mehri, N., Chaleshtori, M.H., Halasz, J., Ercisli, S., Koubouris, G.C., 2018. Interactive effects of temperature and genotype on almond (Prunus dulcis L.) pollen germination and tube length. Sci. Hortic. 227, 162-168.

Sorkheh, K., Shiran, B., Rouhi, V., Khodambashi, M., Wolukau, J.N., Ercisli, S., 2011. Response of in vitro pollen germination and pollen tube growth of almond (Prunus dulcis Mill.) to temperature, polyamines and polyamine synthesis inhibitor. Biochem. Syst. Ecol. 39, 749–757.

Srinivasan, A., Saxena, N., Johansen, C., 1999. Cold tolerance during early reproductive growth of chickpea (Cicer arietinum L.): genetic variation in gamete development and function. Field Crop Res. 60, 209–222.

Ünal, M., Vardar, F., Aytürk, Ö., 2013. Callose in plant sexual reproduction, in: M. Silva-Op (Eds.), Current Progress in Biological Research, Intech Open, pp. 2969.

Voyiatzsis, D.G., Paraskevopoulou-Paroussi, G., 2005. Factors affecting the quality and in vitro germination capacity of strawberry pollen. Int. J. Fruit Sci. 5, 25–35.

Wang, C.L., Wu, J., Xu, G.H., Gao, Y.B, Chen, G., Wu, J.Y., Wu, H.Q., Zhang, S.L., 2010. S-RNase disrupts tip-localized reactive oxygen species and induces nuclear DNA degradation in incompatible pollen tubes of Pyrus pyrifolia. J. Cell Sci. 123, 4301–4309.

Wang, W., Sheng, X., Shu, Z., Li, D., Pan, J., Ye, X., Chang, P., Li, X., Wang, Y., 2016. Combined cytological and transcriptomic analysis reveals a nitric oxide signaling pathway involved in cold-inhibited Camellia sinensis pollen tube growth. Front. Plant Sci. 7, 456.

Wilkins, K.A, Bosch, M., Haque, T., Teng, N., Poulter, N.S., Franklin-Tong, V.E., 2015. Self-incompatibility-induced programmed cell death in field poppy pollen involves dramatic acidification of the incompatible pollen tube cytosol. Plant Physiol. 167, 766-779.

Winship, L.J., Rounds, C., Hepler, P.K., 2017. Perturbation analysis of calcium, alkalinity and secretion during growth of lily pollen tubes. Plants 6, 3.

Wolukau, J.N., Zhang, S., Xu, G., Chen, D., 2004. The effect of temperature, polyamines and polyamine synthesis inhibitor on in vitro pollen germination and pollen tube growth of Prunus mume. Sci. Hortic. 99, 289-299.

Wu, J., Jin, C., Qu, H., Jiang, X., Wu, J., Xu, G., Zhang, S., 2012. The activity of plasma membrane hyperpolarization-activated Ca 2+ channels during pollen development of Pyrus pyrifolia. Acta Physiol. Plant. 34, 969-975.

Wu, J., Shang, Z., Wu, J., Jiang, X., Moschou, P.N., Sun, W., Roubelakis- Angelakis, K.A., Zhang, S., 2010. Spermidine oxidase-derived H2O2 regulates pollen plasma membrane hyperpolarization-activated Ca2+-permeable channels and pollen tube growth. Plant J. 63, 1042-1053.

Yu, Z., Yang, Z., 2019. Understanding different regulatory mechanisms of proteinaceous and non-proteinaceous amino acid formation in tea (Camellia sinensis) provides new insights into the safe and effective alteration of tea flavor and function. Crit. Rev. Food Sci. Nutr. 60, 844-858.

Zhan, H., Nie, X., Zhang, T., Li, S., Wang, X., Du, X., Tong, W., Song, W., 2019. Melatonin: a small molecule but important for salt stress tolerance in plants. Int. J. Mol. Sci. 20, 709.

Zonia, L., 2010. Spatial and temporal integration of signalling networks regulating pollen tube growth. J. Exp. Bot. 61, 1939-1957.

Figure legends

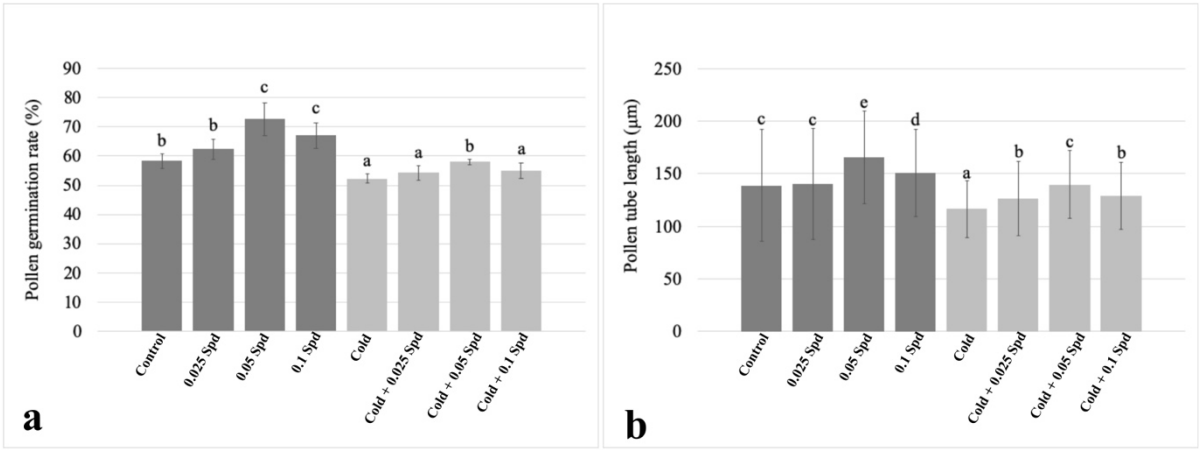

Fig. 1. Effect of Spd treatment, cold stress and Spd treatment concomitant with cold stress. (a) Pollen germination rate (%), (b) pollen tube length (µm). Distinct letters point out the statistically significant differences ($P < 0.05$) and error bars indicate the standard deviations.

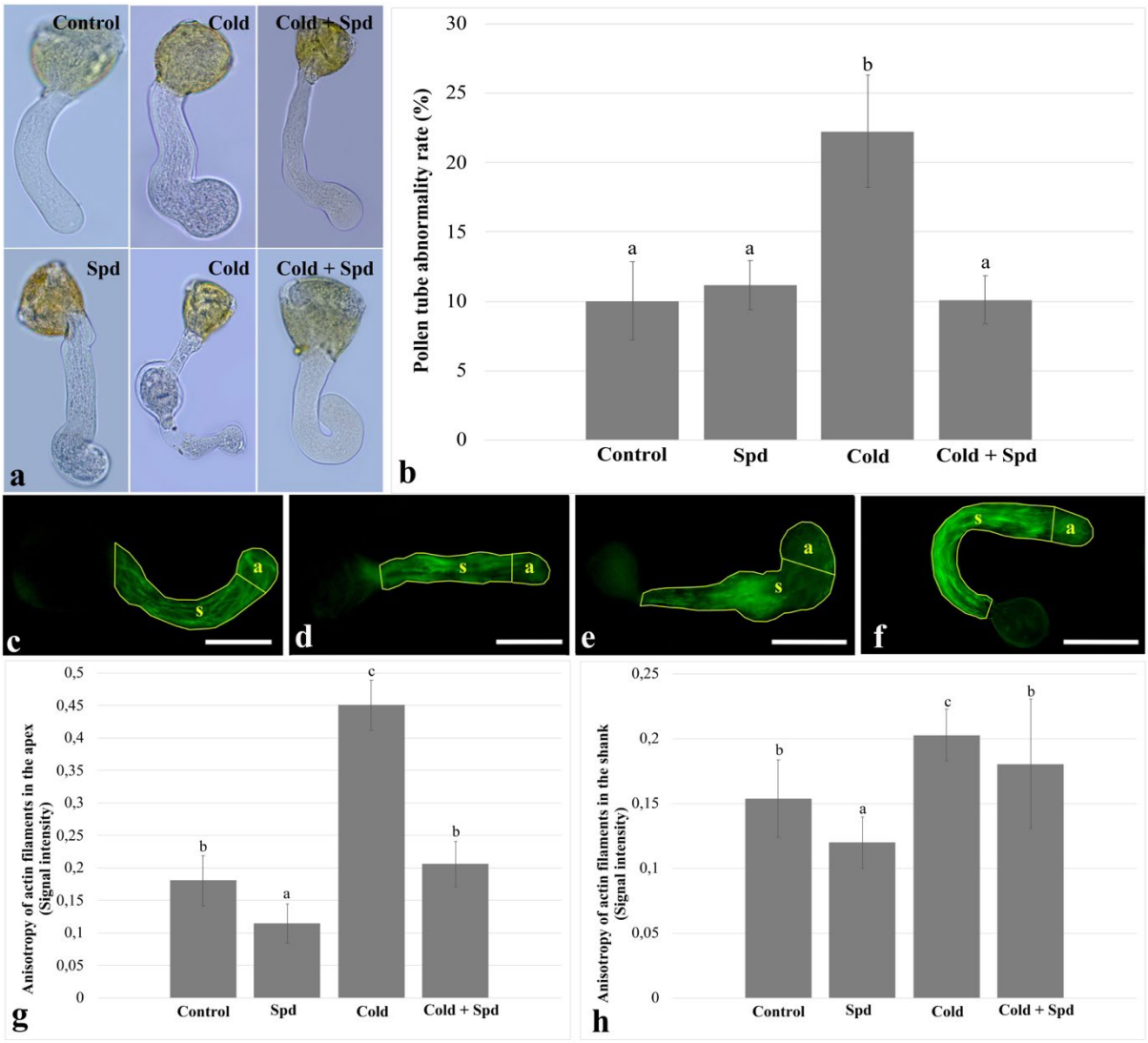

Fig. 2. Pollen tube abnormality and actin filament distribution. (a) Representative images of pollen tube abnormalities, (b) Tube abnormality rates (%), (c) Representative image of actin filament orientation in control group, (d) Representative image of actin filament orientation in Spd-treated group (e) Representative image of actin filament orientation in cold stressed group, (f) Representative image of actin filament orientation in Spd-treated group under cold stress, (g) Actin filament anisotropy in the apex, (h) Actin filament anisotropy in the shank. Apex (a) and shank (s) regions were indicated in the images. Bar: 20 µm. Images are representative of typical experimental cases. Distinct letters point out the statistically significant differences ($P< 0.05$) and error bars indicate the standard deviations.

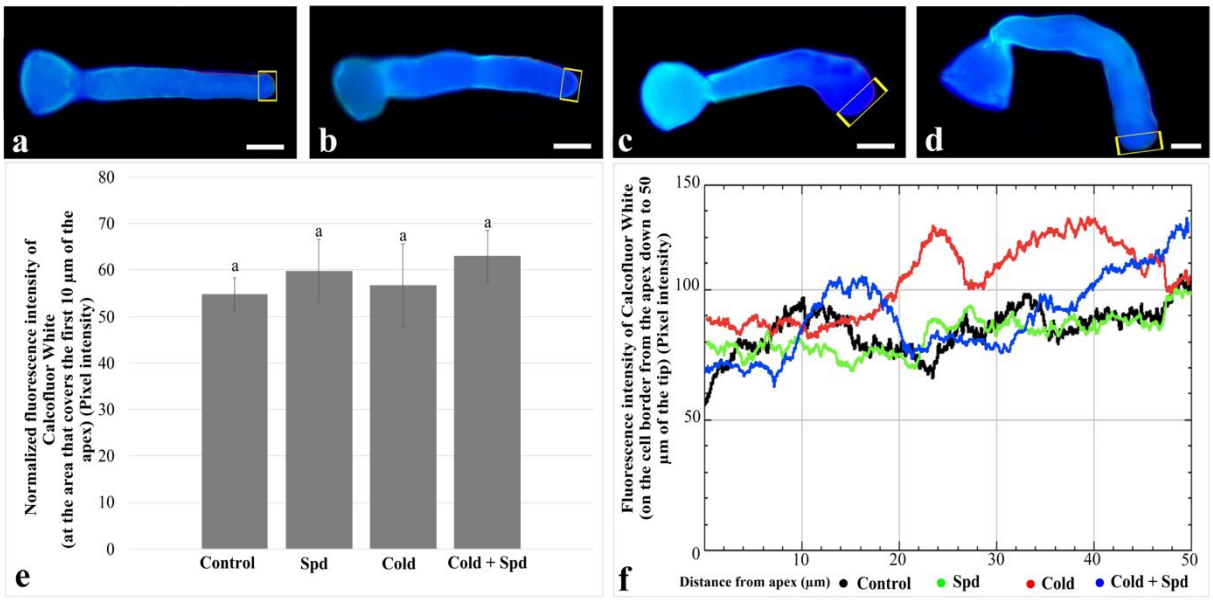

Fig. 3. Cellulose distribution in the pollen tube cell wall. (a) Control, (b) Spd treatment, (c) Cold stress, (d) Spd treatment concomitant with the cold stress, (e) Fluorescence intensity of Calcofluor White as measured in the area corresponding to the first 10 µm of each apex (indicated as box), (f) Graph of fluorescence intensity of Calcofluor White throughout the pollen tube edge from the apex down to 50 µm (indicated as red line). Bar: 20 µm. Images are representative of typical experimental cases. Distinct letters point out the statistically significant differences ($P< 0.05$) and error bars indicate the standard deviations.

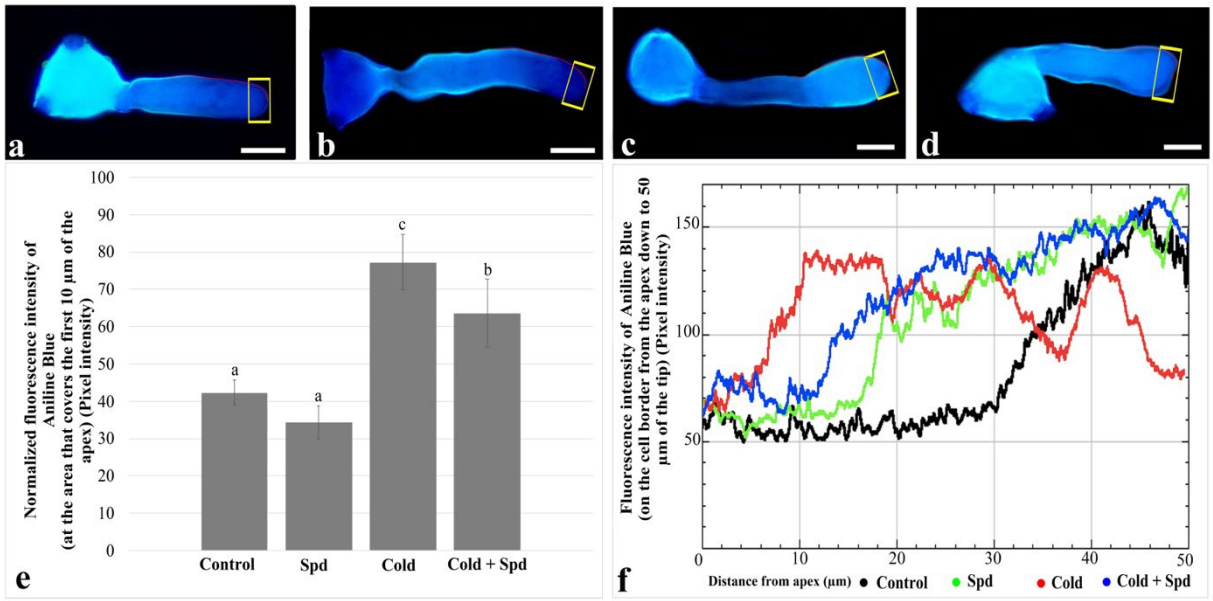

Fig. 4. Callose distribution on the pollen tube cell wall. (a) Control, (b) Spd treatment treatment, (c) Cold stress, (d) Spd treatment concomitant with the cold stress, (e) Fluorescence intensity of Aniline Blue in the area corresponding to the first 10 µm of each apex (indicated by box), (f) Graph of fluorescence intensity of Aniline Blue throughout the pollen tube edge from the apex down to 50 µm (indicated as red line). Bar: 20 µm. Images are representative of typical experimental cases. Distinct letters point out the statistically significant differences ($P< 0.05$) and error bars indicate the standard deviations.

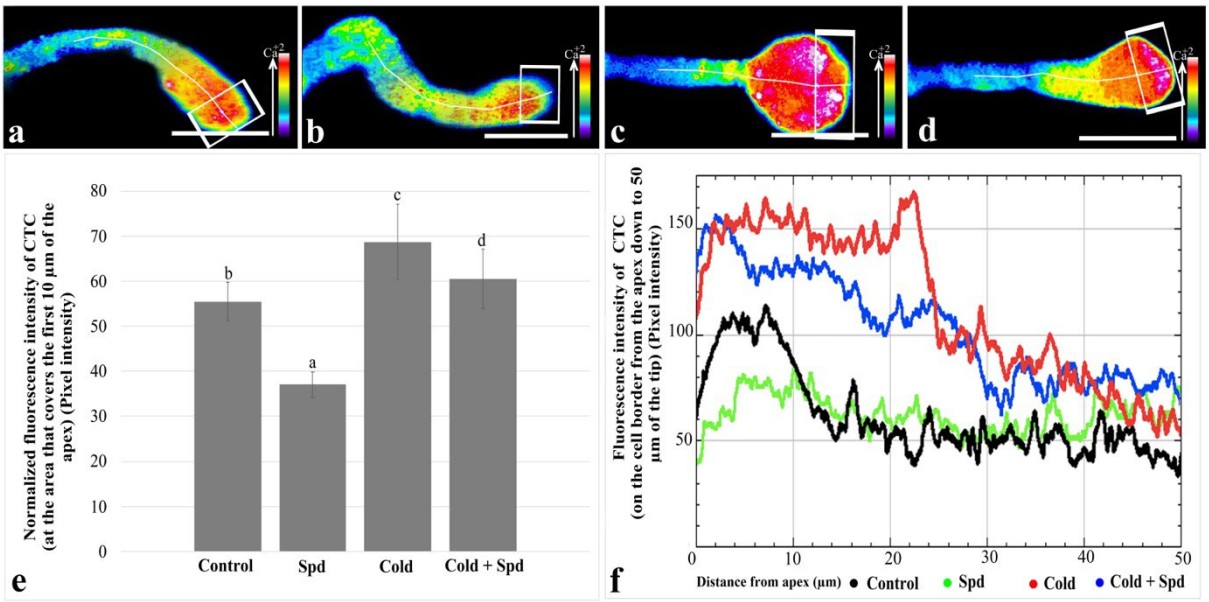

Fig. 5. Changes of Ca^{2+} gradient in the pollen tube. (a) Pseudocolored image of Ca^{2+} -gradient in control group, (b) Pseudocolored image of Ca^{2+}-gradient after Spd treatment, (c) Pseudocolored image of Ca^{2+}-gradient after cold stress, (d) Pseudocolored image of Ca^{2+}-gradient after Spd treatment concomitant with the cold stress, (e) Fluorescence intensity of CTC in the area that covers the first 10 µm of each apex (indicated as box), (f) Graph of fluorescence intensity of CTC throughout the tube, beginning from the outermost tip of the tube to 50 µm behind the tube tip (indicated as red line). Bar: 20 µm. Images are representative of typical experimental cases. Distinct letters point out the statistically significant differences ($P< 0.05$) and error bars indicate the standard deviations.

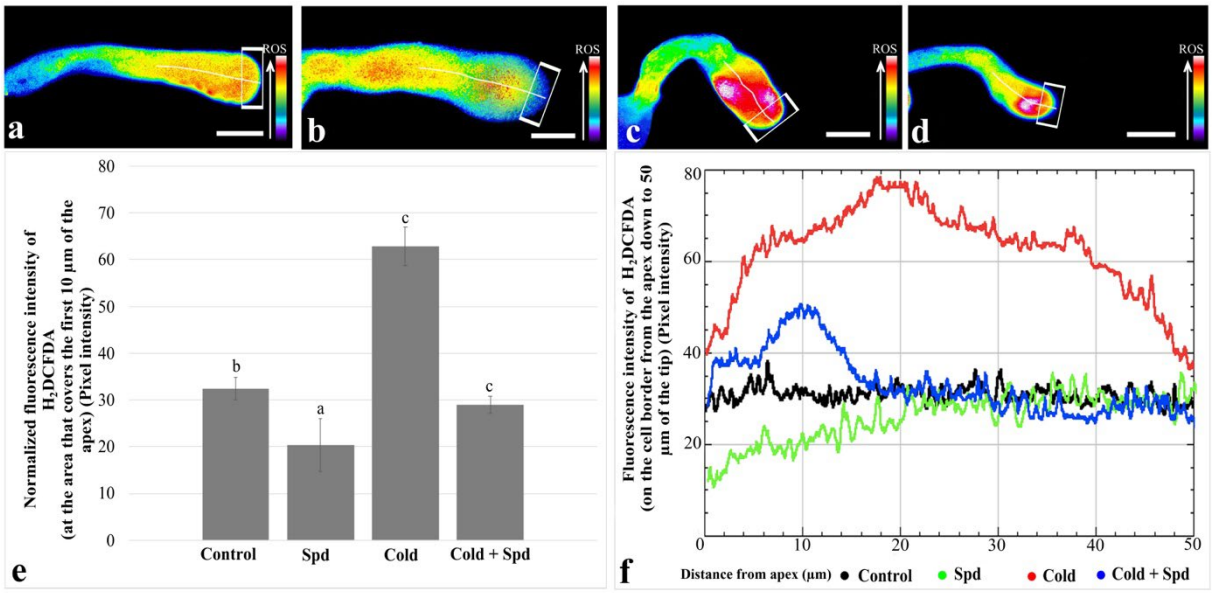

Fig. 6. Changes of ROS accumulation in the pollen tube. (a) Pseudocolored image of ROS accumulation in control, (b) Pseudocolored image of ROS accumulation after Spd treatment, (c) Pseudocolored image of ROS accumulation after cold stress, (d) Pseudocolored image of ROS accumulation after Spd treatment concomitant with the cold stress, (e) Fluorescence intensity of H_2DCFDA in the area that covers the first 10 µm of each apex (indicated as box), (f) Graph of fluorescence intensity of H_2DCFDA throughout the tube, beginning from the outermost tip of

the tube to 50 µm behind the tube tip (indicated as red line). Bar: 20 µm. Images are representative of typical experimental cases. Distinct letters point out the statistically significant differences (P< 0.05) and error bars indicate the standard deviations.

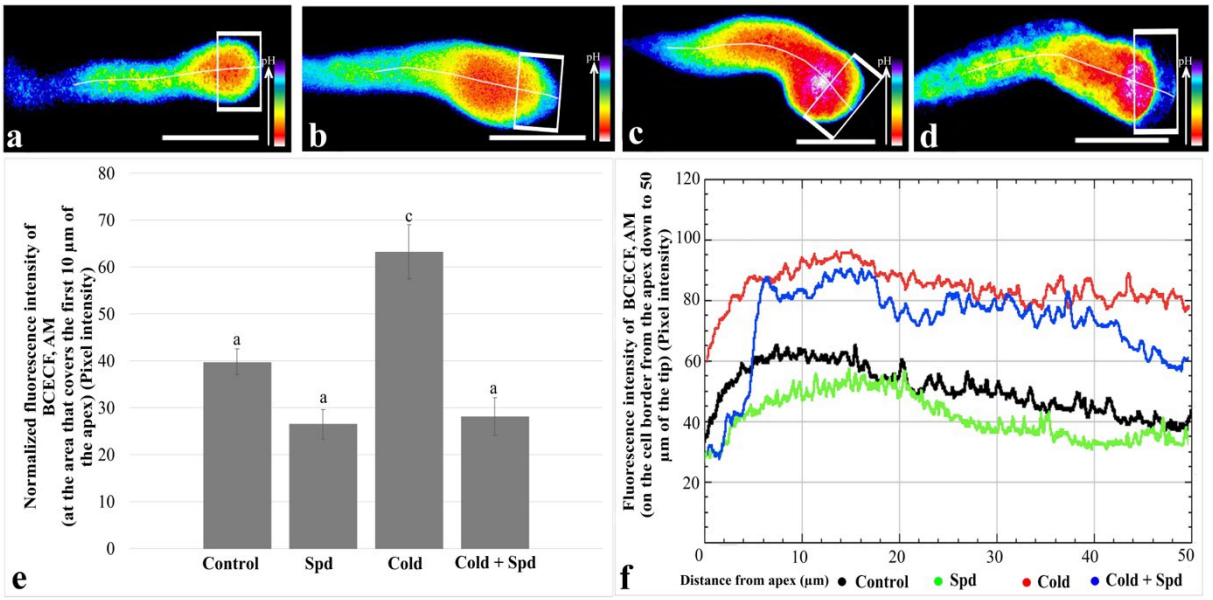

Fig. 7. Changes of pH gradient in the pollen tube. (a) Pseudocolored image of pH gradient in control group, (b) Pseudocolored image of pH gradient after Spd treatment, (c) Pseudocolored image of pH gradient after cold stress, (d) Pseudocolored image of pH gradient after Spd treatment concomitant with the cold stress, (e) Fluorescence intensity of BCECF,AM in the area that covers the first 10 µm of each apex (indicated as box), (f) Graph of fluorescence intensity of BCECF-AM throughout the tube, beginning from the outermost tip of the tube to 50 µm behind the tube tip (indicated as red line). Bar: 20 µm. Images are representative of typical experimental cases. Distinct letters point out the statistically significant differences (P< 0.05) and error bars indicate the standard deviations.

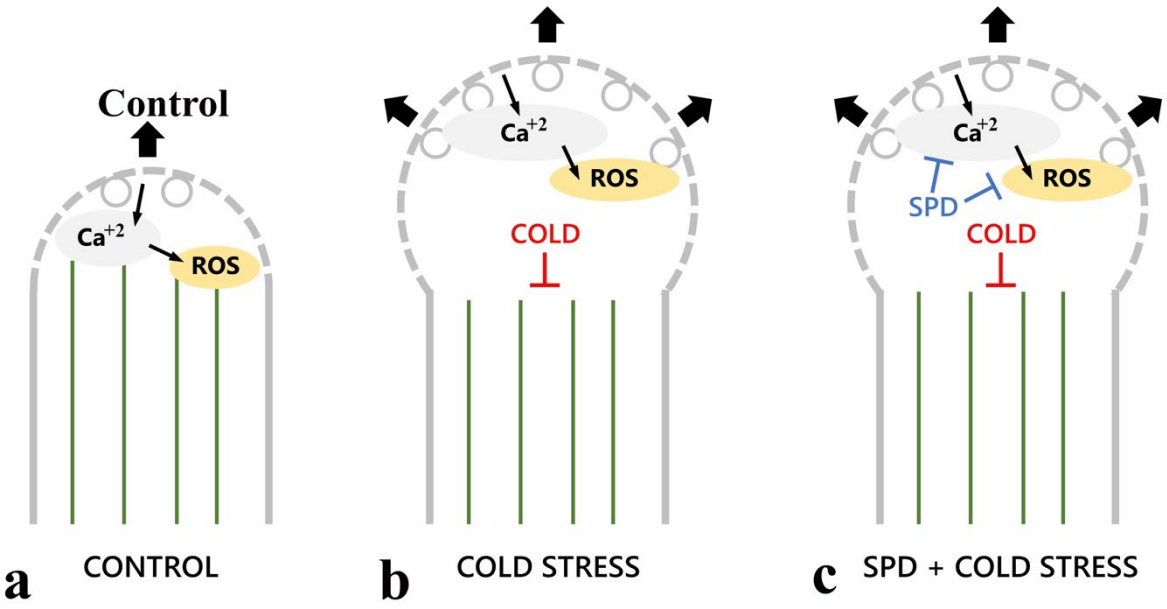

Fig. 8. Illustrative diagram of the current working hypothesis. (a) In the control pollen tubes, the growth process requires that tube elongation (in turn mediated by vesicular secretion and apical cell wall softening) has an effect on the Ca2+ gradient and ROS content, which in turn regulate the dynamics of actin filaments, (b) After cold stress, the disorganization of actin filaments induced by the cold treatment causes an irregular and more delocalized fusion of secretory vesicles with consequent apical swelling and an increase in Ca2+ ion and ROS content, (c) After Spd treatment concomitantly with cold stress would counteract the Ca2 ion and ROS content thereby rebalancing the organization of actin filaments and restoring, at least partially, the correct growth of pollen tubes.